A structural and vibrational study on the first condensed borosulfate $K_5[B(SO_4)_4]$ by using the FTIR–Raman spectra and DFT calculations

Henning Alfred Höppe [a], Karolina Kazmierczak [a], Elida Romano [b], Silvia Antonia Brandán [b,*]

[a] Institut für Physik, Universität Augsburg, Universitätstraße 1, D-86159 Augsburg, Germany
[b] Cátedra de Química General, Facultad de Bioquímica, Química y Farmacia, Universidad Nacional de Tucumán, Ayacucho 471, 4000, San Miguel de Tucumán, Tucumán, Argentina

HIGHLIGHTS

- The first borosulfate, $K_5B(SO_4)_4$ was characterized by IR and Raman spectroscopies.
- DFT calculations were used to study it structure and vibrational properties.
- A complete assignment of the IR and Raman spectra for $K_5B(SO_4)_4$ was performed.
- The nature of the K—O, K—S, B—O, and S—O bonds were analyzed by NBO study.
- The topological properties of the compound were investigated by AIM analysis.

GRAPHICAL ABSTRACT

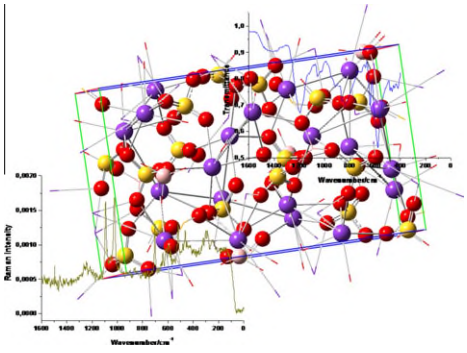

1. Introduction

In this work, as part of our studies on inorganic compounds that containing transition metals with different ligands [1–8], the structural and vibrational properties of the first crystalline borosulfate are presented. Potassium borosulfate, $K_5[B(SO_4)_4]$, recently reported by Höppe et al. [9] was synthesized by heating potassium sulfate with boric and sulfuric acids and contains non-condensed $[B(SO_4)_4]^{5-}$ anions. In that work the compound was characterized by its infrared and Raman spectra but the observed bands in both spectra were not assigned based on a quantum chemical approach.

* Corresponding author. Tel.: +54 381 4247752; fax: +54 381 4248169.
E-mail address: sbrandan@fbqf.unt.edu.ar (S.A. Brandán).

This compound is particularly interesting because the SO_4^{2-} group is a versatile ligand and can act as monodentate or bidentate ligand [5]. Thus, the mode of coordination adopted by the sulfate groups and the stereochemistry of $K_5[B(SO_4)_4]$ are important in relation to its vibrational properties and chemical reactivity. Here, as a contribution to the characterization of this interesting substance, we present a detailed study on the vibrational spectra of this compound and a normal coordinate analysis based on the proposed assignment of bands. The goal of this paper is to perform an experimental and theoretical study on this compound with the methods of quantum chemistry in order to acquire knowledge about its structural and vibrational properties and carry out its complete vibrational assignment. For this purpose, the optimized geometries and frequencies for $K_5[B(SO_4)_4]$ were calculated at B3P86 and B3LYP theory levels. In accordance with the crystal structure determined by Höppe et al. [9] using X-ray diffraction, in the vibrational analysis we have considered this experimental structure of $K_5[B(SO_4)_4]$ as starting point. We intend to show that the DFT normal mode assignments, in terms of the potential energy distribution, are in agreement with those obtained from the normal coordinate analysis. The force fields for the compound were obtained combining the normal modes calculations with a generalized valence force field (GVFF) [10]. In addition, the nature of the different types of K—O, K—S, B—O, and S—O bonds and the topological properties of the electronic charge density, were performed by means of NBO [11] and AIM [12,13] calculations. Previously we reported the vibrational spectra and the complete assignments for the new zinc difluoromethanesulfinate salt, $Zn(SO_2CF_2H)_2$ [8]. The difluoromethanesulfinate salt was structural and vibrationally studied by means of normal mode calculations accomplished of a generalized valence force field (GVFF) in order to analyze the coordination modes of the difluoromethanesulfinate groups and carry out their complete assignments [8]. In this paper, we extend our investigation to a compound that contains a B atom in the structure which is classed as a metalloid. Here, the structural and vibrational properties for the first crystalline borosulfate are presented and analyzed.

2. Experimental

In the present work the $K_5[B(SO_4)_4]$ has been synthesized according to Höppe et al. [9]. The infrared spectrum of potassium borosulfate in the wavenumbers range from 4000 to 400 cm^{-1} was collected at room temperature by using a Bruker EQUINOX 55 FTIR-spectrometer, the Raman spectrum was recorded by a Bruker FRA 106/S module with a Nd—YAG laser (λ = 1064 nm) scanning a range from 4000 to 10 cm^{-1}.

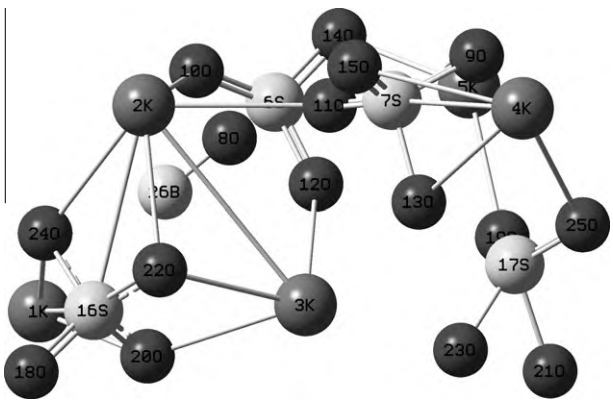

Fig. 1. Theoretical structure and labelling of the atoms for potassium borosulfate, $K_5[B(SO_4)_4]$.

3. Computational details

The starting points for the geometric optimizations of the potassium borosulfate structure were taken from those experimentally determined from single-crystal data using X-ray diffraction [9]. The calculations were carried out with the hybrid B3LYP [14,15] and B3P86 methods [16] together with the 6-31G* basis set. The numbering of the atoms for those structures is described in Fig. 1. In this study, in accordance with the experimental results, the symmetry adopted by three sulfate groups of this compound was C_{3v} while that adopted for the remaining group was C_{2v}. Thus the natural coordinates for the potassium borosulfate structure are similar to those reported in the literature [1–5,17–24] as can be seen in Table S1 of the Supporting material. The title compound comprises various fused rings. Therefore, for the treatment of the internal coordinates four rings were considered for potassium borosulfate, two consisting of four members [1–5], one of five members [17–20] and another of six members [21–24]. Detailed structural information from each ring is shown in Fig. S1 (Supporting information). The normal mode analyses for the optimized structures were carried out with the B3P86/6-31G* and B3LYP/6-31G* methods. The harmonic force fields in Cartesian coordinates which resulted from the calculations were transformed to "natural" internal coordinates by using the MOLVIB program [25]. The Potential Energy Distribution (PED) components were subsequently calculated with the resulting scaled quantum mechanics (SQMs) force field. The complete assignment of the potassium borosulfate was performed by means of *GaussView* program [26]. In addition, for $K_5[B(SO_4)_4]$ by using the B3P86/6-31G* and B3LYP/6-31G* methods, the atomic charges, bond order expressed as Wiberg indices, main delocalization energy and the frontier molecular HOMO and LUMO orbitals were calculated and analyzed. The electronic charge density topological analysis was performed by using the AIM methodology [12] and the AIM200 program package [13] while the NBO calculation was carried out by using the NBO 3.1 program [27], as implemented in the GAUSSIAN 03 package [28].

4. Results and discussion

4.1. Geometry calculations

Table S2 (Supporting material) shows a comparison of the total energies and dipole moment values for potassium borosulfate by using the B3P86 and B3LYP methods and the 6-31G* basis set. Note that the lower energy value was obtained by using the B3P86/6-31G* combination. Table 1 shows a comparison of the calculated geometrical parameters for the compound with the ones corresponding to those observed from X-ray diffraction [9]. Experimentally, $K_5[B(SO_4)_4]$ crystallizes in a new structure type in the chiral space group $P4_1$. The crystal structure of $K_5[B(SO_4)_4]$ comprises novel, large non-condensed anions $[B(SO_4)_4]^{5-}$ in which a central borate tetrahedron shares all four corners with neighboring sulfate tetrahedra [9]. These central boron atoms adopt an only slightly distorted body-centred packing with the apices of the borate tetrahedra pointing more or less directly along the *c* axis, resulting in a polar crystal structure. The potassium atoms are situated in the voids of the resulting structure, as can be seen in Fig. S2. The theoretical values were compared with the average experimental values reported for the compound by means of the square root mean of deviation (RMSD) values. In general, our theoretical values are in fair agreement with the experimental ones. Note that the terminal

Table 1
Calculated geometrical parameters for $K_5B(SO_4)_4$.

Parameters	6-31G*[a]		Experimental[b]
	B3LYP	B3P86	
Bond length (Å)			
B26—O8	1.288	1.289	1.303
S6—O8	1.792	1.767	1.711
S6—O10	1.464	1.458	1.691
S6—O12	1.475	1.469	1.693
S6—O14	1.467	1.462	1.706
K5—O14	2.796	2.774	2.586
S7—O9	1.498	1.490	1.687
S7—O15	1.479	1.471	1.753
S7—O11	1.489	1.481	1.682
S7—O13	1.641	1.631	1.687
K4—O15	2.817	2.826	2.552
K5—O9	2.747	2.725	2.513
K4—O25	2.667	2.646	2.544
S17—O19	1.476	1.471	1.727
S17—O21	1.711	1.701	1.739
S17—O23	1.619	1.608	1.687
S17—O25	1.473	1.467	1.765
K5—O19	2.676	2.654	2.574
K2—O22	2.588	2.572	2.469
K2—O24	2.649	2.625	2.467
K2—K3	3.944	3.912	3.507
S16—O18	1.476	1.470	1.777
S16—O20	1.541	1.532	1.689
S16—O22	1.528	1.519	1.685
S16—O24	1.540	1.532	1.689
K1—O20	2.591	2.575	2.477
K1—O24	2.598	2.577	2.451
K1—S16	3.106	3.122	3.106
RMSD	0.04	0.04	
Bond angle (°)			
O8—S6—O14	101.9	102.0	110.8
O10—S6—O12	116.9	116.9	120.0
O11—S7—O15	115.8	116.0	132.9
O13—S7—O9	105.7	112.1	99.5
O18—S16—O22	113.3	113.3	117.1
O20—S16—O24	106.0	106.0	102.7
O20—K1—O24	56.6	56.7	64.7
K1—O20—K3	135.9	136.6	108.3
K1—O24—K2	133.8	135.2	115.9
O9—K5—O19	69.7	69.3	75.6
O9—K5—O14	128.4	127.8	152.5
O19—K5—O14	133.8	134.3	78.1
O13—K4—O25	54.0	53.9	66.7
O11—K2—O10	73.6	73.6	68.5
K3—O22—K2	98.8	98.6	89.6
S6—O8—B26	127.7	127.2	134.3
RMSD	4.7	4.8	
Dihedral angles (°)			
K1—O24—K2—O11	−53.8	−53.2	−45.8
K4—O9—K5—O14	145.1	148.5	−15.0
K1—O20—K3—K5	6.6	5.49	11.2
K4—O15—S7—O11	175.2	175.0	179.3
B26—O8—K5—O14	−152.5	−175.6	−26.2
K1—K2—K3—K5	116.7	116.7	104.5
K2—K3—K5—K4	86.0	85.7	117.0
RMSD	29.5	32.0	

[a] This work.
[b] Experimental for $K_5[B(SO_4)_4]$ from Ref. [9].

S—O bonds are shorter than the bridging ones (S—O—B) in the X-ray structure, in contrast to the theoretical values. The difference between the experimental and theoretical results could be attributed to the effect of crystal packing forces acting on $K_5[B(SO_4)_4]$ molecules in the lattice, perturbations not taken into account in the calculations, such as strong S—O···O, S—O···K, K—O···O inter-molecular bonds. Both results provide a reliable starting point for the B3P86/6-31G* or B3LYP/6-31G* force fields and frequency calculations. Three short S—O bonds for the sulfate groups (S6, S7, S16 atoms) with similar distances are justified by the corresponding O—S—O angular deformations of these atoms, and for this reason, they were considered with C_{3v} symmetries. On the other hand, the two pairs of O atoms attached to the S17 atom have approximately the same S—O distances and, for this, another sulfate group (S17) was considered with C_{2v} symmetry. Thus, the best results for bond lengths and angles as well as dihedral angles, by using both methods, with the 6-31G* basis set are obtained. The dihedral angles for the compound show that the B26—O8—K5—O14 dihedral angle, by using both calculation levels, justify the higher differences in the calculated RMSD values, as observed in Table 1.

The stability of the potassium borosulfate structure by using those approximation levels and the 6-31G* basis set was investigated by means of the electronic charge density topological analysis, bond orders and the natural population atomic charge values (NPA). The NPA values are given in Table S3 while the bond order, expressed by Wiberg's indices, for all the atoms of the compound are summarized in Table S4. Notice that the calculated values for each atom by using the B3P86/6-31G* combination are slightly higher than the other ones. Probably, the dipolar moment for the compound by using the B3P86/6-31G* level could partly explain its relative stability, as observed in other molecules [29,30]. The higher NPA charge value is observed on the S7 atom while the lower value on the B26 atom. As expected, the NPA charges on the K atoms have higher positive values than the B atom but lower than the S atoms. The bond orders, for potassium borosulfate by using both calculation levels are shown in Table S4. The total bond orders per atom calculated on both levels show that in potassium borosulfate three sulfate groups comprise four asymmetric bonds. Thus, for the S6 atom, the bond orders for the S6—O8, S6—O10, S6—O12 and S6—O14 bonds are 0.4608, 1.2631, 1.2074 and 1.2598, respectively; for the S7—O13, S7—O9, S7—O11 and S7—O15 bonds the bond orders are 0.7092, 1.1287, 1.1550 and 1.2153, respectively; and, for the S16—O18, S16—O20, S16—O22 and S16—O24 bonds, the bond orders are 1.2111, 0.9993, 1.0232 and 1.0002, respectively. On the other hand, the bond orders calculated for all potassium atoms show values between 0.0846 and 0.2146, indicating the formation of coordination bonds between potassium and oxygen and the S and O atoms. Here, only the O21 and O23 atoms show a partial double bond character in the S17═O21 and S17═O23 bonds with values of bond orders of 1.7344 and 1.9423, respectively, calculated by using the B3P86/6-31G* method.

For potassium borosulfate, the second order perturbation energies $E^{(2)}$ (donor → acceptor) that involve the most important delocalization were analyzed by means of NBO calculations [11] and the results are given in Table S5. The contributions of the stabilization energies to the $\Delta ET_{\sigma^*\rightarrow\sigma^*}$ charge transfers are higher than the corresponding to the $\Delta ET_{LP\rightarrow\sigma^*}$ charge transfers due mainly to the S and O atoms. Thus, this analysis confirms the high stability of this compound with a value of ΔE_{Total} of 19214 kJ/mol. Moreover, the calculated values by using B3P86 calculations are slightly higher than those calculated on the B3LYP level in accordance with the values presented in Table S2.

The intermolecular interactions for the potassium borosulfate structure have been also studied by using *Bader's* topological analysis of the charge electron density, $\rho(r)$ using the AIM program [13]. For the characterization of the molecular electronic structure are important the determination of the $\rho(r)$ in the bond critical points (BCPs) and the values of the Laplacian, $\nabla^2(r)$ at these points. The topological properties of only some BCPs and RCPs for the potassium borosulfate structure with the B3LYP/6-31G* method are reported and compared with the corresponding calculated by using B3P86/6-31G* level in Table S6. The results show two important observations, in one case, the O23---O21, O12---O11,

K1 → B26 and K → O BCPs have the typical properties of closed–shell interactions ($\rho(r) \leqslant 0.07$ a. u., $|\lambda 1|/\lambda 3 < 1$ and $\nabla^2(r) = 0.10$–0.30 a.u.) [29,30] while the other important observation is related to the topological properties of the O13---S17 BCP since in both calculation levels they have approximately the same topological properties. The latter results clearly show that there are important interactions between sulfate groups, i.e. between an O atom of a group with the S atom of another group. The critical points and the ring points of the electron density obtained by AIM analysis for potassium borosulfate are shown in Fig. S3. The results analyzed for the compound are in agreement with the structure observed by X-ray-diffraction experiments and strongly support the conclusions reported previously about the ionic nature of this compound [9].

4.2. Vibrational frequencies

The structure of potassium borosulfate exhibits C_1 symmetry and 72 active vibrational normal modes in both infrared and Raman spectra. Figs. 2 and 3 show the registered infrared and Raman spectra for the compound in the solid phase, respectively. Both experimental spectra are compared with the corresponding calculated ones from B3LYP/6-31G* and B3P86/6-31G* calculations (Figs. 2 and 3). In general, the theoretical infrared and Raman spectra of potassium borosulfate by using the B3P86/6-31G* method demonstrates a better agreement with the experimental spectrum, as observed in Figs. 2 and 3. We have performed this study taking into account the B3P86/6-31G* method and a C_{3v} symmetry for three sulfate groups of this compound while a C_{2v} symmetry for the remaining group, as was described in Section 4.1. The assignment of the experimental bands to the expected normal vibration modes were made on the basis of potential energy distribution components (PEDs) in terms of symmetry coordinates, and by taking into account the assignments of related molecules [5,8,19,31–38]. Table 2 shows the experimental and calculated frequencies by using the B3P86/6-31G* method and the corresponding assignment for potassium borosulfate. Table S7 shows the experimental and calculated frequencies for the compound and the potential energy distribution based on the B3P86/6-31G* level. The PEDs higher than or equal to 10% were subsequently calculated with the resulting SQM. The SQMFF method was performed by using the Pulay's scaling factors defined by the 6-31G* basis set [39]. It is possible to observe that in both calculations some vibrational modes related to the rings are mixed among them due to the fused rings;

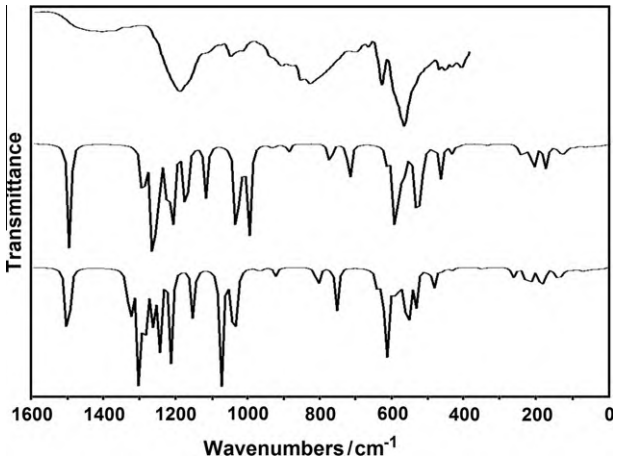

Fig. 2. Upper, experimental infrared spectrum of the solid potassium borosulfate, $K_5[B(SO_4)_4]$ in KBr pellets, Medium; theoretical spectrum by using B3LYP/6-31G* level and; bottom, theoretical spectrum by using B3P86/6-31G* level.

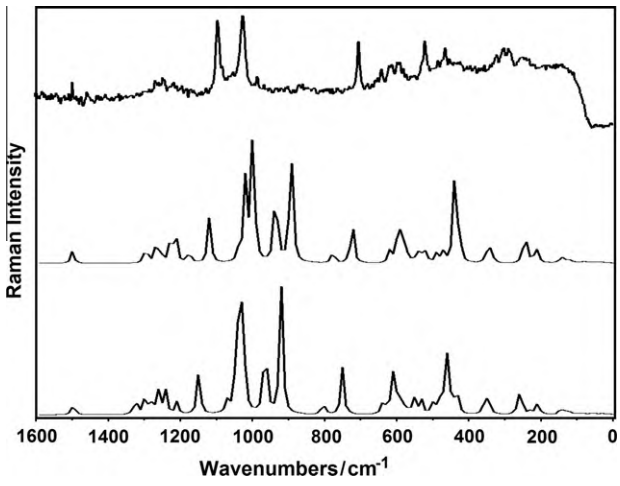

Fig. 3. Upper, experimental Raman spectrum of the solid potassium borosulfate, $K_5[B(SO_4)_4]$ in KBr pellets, medium; theoretical spectrum by using B3LYP/6-31G* level and; bottom, theoretical spectrum by using B3P86/6-31G* level.

thus, those vibrational modes are restricted and observed with low PED values. In these cases, the final assignment was performed with the aid of *GaussView* program [26]. The calculated harmonic force field for the compound studied can be obtained upon request. Below we discuss the assignment of the most important groups.

4.2.1. B—O—S group

In borates, such as pure boron oxide glasses [32], the strong band around 1276 cm^{-1} and the shoulders at 1492 cm^{-1} are assigned to the B—O stretching modes while the corresponding B—O—B deformation mode is recorded at 656 cm^{-1}. In potassium borosulfate, the B—O stretching mode is predicted by calculations with a PED contribution of 89% and, for this reason, it is easily assigned to the Raman band of the medium intensity at 1494 cm^{-1} while the S—O mode is predicted with a low PED value and, hence, with aid of the *GaussView* program [26] its mode is assigned to the IR and Raman bands at 467 and 483 cm^{-1}, respectively. The calculations predict the B—O—S deformation mode in the low frequencies region with a PED contribution of 44% and coupled with other modes, thus, the very weak Raman band at 199 cm^{-1} is assigned to that mode.

4.2.2. Sulfate groups

In compounds containing tetrahedral sulfate groups [34–37], the expected asymmetric, symmetric stretching and bending modes are found in the 1150 and 320 cm^{-1} region. In potassium borosulfate, for each sulfate group with C_{3v} symmetry three SO_3 stretching modes are expected, two modes of which are antisymmetric and one symmetric. They were assigned to the bands around 1375 and 884 cm^{-1} (Table 2). The two pairs of shoulders and bands in the IR and Raman spectra at 1337/1092 and 946/547 cm^{-1}, respectively, in accordance with similar compounds [8,19] and by calculations, are associated with the SO_2 antisymmetric and symmetric stretching modes corresponding to the sulfate group with C_{2v} symmetry, as can be seen in Table 2. Notice that the symmetric stretching modes are predicted in the Raman spectrum with higher intensity than expected. Here, the antisymmetric and symmetric bending modes are predicted by calculations between 724 and 520 cm^{-1}; for this reason, they were assigned in this region. The rocking and twisting modes are clearly predicted in the expected regions [38] for the three sulfate groups of potassium borosulfate, thus, they were assigned in those regions, as observed in Table 2. Here, only the SO_2 vibration modes

Table 2
Observed and calculated wavenumbers (cm^{-1}) and assignment for $K_5B(SO_4)_4$.

Modes	IR[a]	Raman[a]	Calc.[b]	IRc int.[c]	Raman[d] act.	SQM[e]	Assignment[a]
1	1409 w	1494 m	1504	422.5	3.1	1445	ν (B26—O8)
2	1375 sh	1268 w	1323	289.8	4.3	1281	ν_{as} SO_3(S6)
3	1337 sh	1255 w	1298	469.3	3.5	1248	ν_{as} SO_2(S17)
4	1258 sh	1246 w	1283	358.7	3.9	1234	ν_{as} SO_3(S6)
5		1214 w	1261	221.4	6.4	1214	ν_{as} SO_3(S7)
6	1195 s	1190 w	1241	371.5	6.9	1195	ν (S16—O18)
7	1182	1165 vw	1209	387.0	3.1	1165	ν_{as} SO_3(S7)
8	1083 sh	1092 vs	1148	218.9	10.6	1105	ν_s SO_2(S17)
9	1056 m	1048 vw	1069	487.9	2.9	1033	ν_{as} SO_3(S16)
10	1023 m	1022 vs	1043	90.9	24.2	1019	ν_s SO_3(S6)
11		1004 sh	1033	347.6	2.9	995	ν_{as} SO_3(S16)
12	972 sh	984 w	1027	24.3	32.1	984	ν_s SO_3(S7)
13	946 sh	963 w	965	19.0	21.2	942	ν_s SO_2(S17)
14	884 m	884 vw	920	35.4	32.3	884	ν_s SO_3(S16)
15	837 s		803	101.8	3.1	783	ν (S7—O13)
16	705 m	703 s	750	181.6	12.1	724	δSO_2(S17)
17	640 s	638 m	636	115.7	4.1	638	ρSO_3(S7)
18	610 sh	610 m	614	286.0	3.6	609	$\delta_s SO_3$(S6)
19		595 m	609	201.9	8.2	602	$\delta_s SO_3$(S7)
20	598 sh	595 m	599	14.9	2.9	595	$\delta_a SO_3$(S16)
21	578 vs	587 m	591	37.9	1.1	587	$\delta_a SO_3$(S16)
22		577 sh	587	49.2	2.3	583	$\delta_s SO_3$(S16)
23		570 sh	575	94.7	1.9	570	$\delta_a SO_3$(S7)
24	549 sh	547 vw	554	352.4	1.4	548	$\delta_a SO_3$(S6), ν_{as} SO_2(S17)
25		526 sh	549	7.4	3.1	538	τR_2 (A4)
26	518 sh	520 s	533	64.6	0.8	530	$\delta_a SO_3$(S6), τwSO_2(S17)
27		520 s	531	111.9	3.0	516	$\delta_a SO_3$(S7)
28	481 m	506 sh	497	13.1	3.1	493	ρSO_2(S17), $wagSO_2$(S17),
29	467 m	483 m	482	91.5	3.1	470	τwSO_2(S17), ν (S6—O8)
30	457 sh	462 s	462	14.9	17.0	451	δSO_2(S17)
31	446 m		451	5.1	2.6	445	δSO_2(S17), βR_2 (A4), τR_2 (A4)
32		450 m	442	0.1	1.5	442	ρSO_3(S16)
33	424 sh	438 w	435	2.4	1.9	433	βR_1 (A4), ρSO_3(S16)
34	420 m	421 w	431	8.7	3.2	431	ν_s (K—O)
35		379 w	360	0.6	1.4	364	ν_s (K5—O), ρSO_3(S6)
36		353 w	349	3.6	2.9	350	βR_2 (A4)
37		338 sh	344	4.1	2.7	343	ρSO_3(S6), Butt
38		300 m	261	40.5	3.8	260	ρSO_3(S7)
39		286 m	254	8.9	3.8	247	βR_1 (A4)
40		238 w	230	5.9	0.2	223	τR_1 (A3)
41		220 sh	228	6.0	0.3	220	ν(K—O)
42		213 sh	226	41.8	0.5	218	ν_a (K—O)
43		199 vw	214	74.3	0.2	208	δ(B26—O8—S6)
44		199 vw	209	9.5	2.9	204	ν_s (K—O)
45		191 vw	187	31.6	0.05	194	βR_1 (A2)
46		188 vw	183	76.8	0.	181	ν_s (K—O)
47		161 vw	170	19.2	0.06	164	δ(O12—K5—O14)
48		154 vw	149	9.5	0.6	152	δ(O12—K5—O14), ν_a(K5—O), βR_1 (A4)
49		139 vw	143	0.5	0.2	139	ν_a(K5—O), τwSO_3(S6)
50		133 sh	141	14.3	0.5	136	ν_s (K—O)
51		133 sh	135	33.7	0.6	132	ν(K4—O25)
52		123 sh	134	1.9	0.1	124	ν_s (K5—O)
53		116 sh	130	16.3	0.1	119	δ(O12—K5—O14), τR_2 (A4)
54		116 sh	124	2.5	0.5	114	βR_1 (A4)
55		106 sh	119	7.6	0.2	107	τwSO_3(S16)
56		106 sh	113	7.3	0.2	105	γ S7—O11
57		106 sh	102	5.4	0.2	100	βR_2 (A4), δ(O12—K5—O14)
58		91 sh	95	7.6	0.2	91	ν(K—O)
59		91 sh	91	3.1	0.1	90	ν(K—O)
60		76 sh	80	0.7	0.3	77	ν(K—O)
61		76 sh	74	7.8	0.1	72	τR_2 (A2)
62		67 sh	73	7.9	0.1	72	δ(O9—K5—O14), τR_1 (A1)
63		67 sh	66	2.0	0.03	64	τR_3 (A4)
64		56 sh	58	2.5	0.1	58	δ(O11—K2—O22)
65		56 sh	57	6.9	0.1	56	τR_1 (A2)
66		45 vw	52	3.8	0.1	49	τR_1 (A4)
67		45 vw	48	1.5	0.05	44	βR_1 (A3)
68		30 vw	35	9.2	0.2	35	δ(O12—K5—O14), τR_2 (A4)

Table 2 (*continued*)

Modes	IR[a]	Raman[a]	Calc.[b]	IRc int.[c]	Raman[d] act.	SQM[e]	Assignment[a]
69		30 vw	31	2.5	0.1	29	βR_2 (A2)
70		30 vw	29	1.2	0.1	26	τwSO_3(S7)
71		**20**	20	2.9	0.1	20	Butt
72		**10**	10	4.2	0.2	10	βR_1 (A2)

Abbreviations: ν, stretching; β, deformation in the plane; γ, deformation out of plane; wag, wagging; τ, torsion; β_R, deformation ring τ_R, torsion ring; ρ, rocking; twis, twisting; α, angular deformation; δ, deformation; Butt, butterfly; a, antisymmetric; s, symmetric; A1, Ring 1 (five members); A2, Ring 2 (four members); A3, Ring 3 (four members) and A4, Ring 4 (six members).

The bold letters are the theoretical values considered as experimental ones.

[a] This work.

[b] B3P86/6-31G* level.

[c] Units are km mol^{-1}.

[d] Raman activities in $Å^4$ $(amu)^{-1}$.

[e] From SQM B3LYP/6-31G*.

corresponding to the O21—S17—O23 bond angle were considered because the other SO_2 group is included into the A2 ring (see Fig. S1). Thus, the shoulder and the Raman bands at 506, 483 and 462 cm^{-1} are respectively assigned to the rocking, twisting and bending modes of that group, as observed in Table 2. The SO_2 wagging was not predicted in the PED contribution (see Table S7), for this, it was assigned with aid to the *GaussView* program [26] coupled with the rocking mode at 481 cm^{-1}.

4.2.3. O—K—O group

Theoretically, the K—O stretching modes are predicted, with low PED contribution and coupled with other modes, in the lower wavenumbers region, i.e. in the region between 420 and 76 cm^{-1}. Thus, those modes are assigned as can be seen in Tables 2 and S7. On the other hand, the deformation modes corresponding to the O12—K5—O14, O9—K5—O14 and O11—K2—O22 bond angles are assigned respectively to the shoulder in the Raman spectrum at 161, 67 and 56 cm^{-1}.

4.2.4. Skeletal modes

In potassium borosulfate, the description of the skeletal stretching modes appears to be strongly mixed among them as can be seen in Table 2. Taking into consideration their relative position, intensities predicted by calculations, the expected deformations and torsions modes corresponding to the considered A1, A2, A3 and A4 rings were assigned as observed in Table 2. The remaining skeletal modes were assigned according to PED contribution, as can be seen in Tables 2 and S7.

4.3. HOMO–LUMO energy gap

The frontier molecular HOMO and LUMO orbitals for potassium borosulfate were calculated by using both calculation levels, as observed in Table S8. The results show that both orbitals are mainly localized on the p_y and p_z orbitals of the oxygen atoms and that the values of the energy separation between those orbitals are higher by using the B3P86/6-31G* level. This is in accordance with the high stability observed by NBO calculations. These large HOMO–LUMO gaps (−3.19 and −3.70 eV by using both levels) for the compound automatically mean good stability and especially a high chemical hardness.

5. Conclusions

The first crystalline borosulfate, $K_5[B(SO_4)_4]$, was characterized by infrared and Raman spectroscopy in the solid phase. The theoretical molecular structures of $K_5[B(SO_4)_4]$ were determined by the B3LYP/6-31G* and B3P86/6-31G* methods. The calculated harmonic vibrational frequencies by using the B3P86/6-31G* method for the potassium borosulfate compound are consistent with the experimental IR and Raman spectra. An SQM/B3P86/6-31G* force field was applied for adjusting the obtained theoretical force constants, and to minimize the difference between the observed and calculated wavenumbers. The nature of the K—O, K—S, B—O, and S—O bonds and the topological properties of the compound were investigated and analyzed by means of Natural Bond Order (NBO) and *Bader's* Atoms in Molecules theory (AIM), respectively. The NBO and AIM results for the compound are in good agreement with the crystal structure based on X-ray-diffraction data. Our results strongly support the conclusions reported previously about the ionic nature of this compound. The HOMO–LUMO study reveals the high chemical hardness of the title compound.

Acknowledgements

This work was funded with grants from CIUNT (Consejo de Investigaciones, Universidad Nacional de Tucumán). The authors thank Prof. Tom Sundius for his permission to use MOLVIB.

Appendix A. Supplementary material

Supplementary data associated with this article can be found, in the online version, at http://dx.doi.org/10.1016/j.molstruc.2012.12.042.

References

[1] S.A. Brandán, M.L. Roldán, C. Socolsky, A. Ben Altabef, Spectrochim. Acta Part A 69 (2008) 1027.
[2] S.A. Brandán, C. Socolsky, A. Ben Altabef, Z. Anorg, Allg. Chem. 635 (3) (2009) 582.
[3] S.A. Brandán, J. Mol. Struct. (THEOCHEM) 908 (2009) 19.
[4] S.A. Brandán, Structural and vibrational properties of chromyl perchlorate, in: Perchlorates: Production, Uses and Health Effects, Edited Collection, Nova Science Publishers, Inc., ISBN: 978-1-61761-812-3, 2010 (Chapter 9).
[5] A. Ben Altabef, S.A. Brandán, J. Mol. Struct. (2010) 146.
[6] M.V. Castillo, E. Romano, H.E. Lanús, S.B. Díaz, A. Ben Altabef, S.A. Brandán, J. Mol. Struct. 994 (2011) 202.
[7] S.A. Brandán, Structural and vibrational investigation of nitrate compounds combining FTIR-Raman and DFT calculations, in: Nitrate: Occurrence, Characteristics and Health Considerations, Edited Collection, Nova Science Publishers, Inc., ISBN: 978-1-62257-352-3, Data of publication: June, 2012.
[8] E. Romano, S. Locatelli, S.A. Brandán, NBO, AIM and the molecular force field studies on a new compound: the zinc difluoromethanesulfinate salt, in: XXXI European Congress Molecular Spèctroscopy (EUCMOS), September 2012, Cluj-Napoca, Rumania.
[9] H.A. Höppe, K. Kazmierczak, M. Daub, K. Förg, F. Fuchs, H. Hillebrecht, Angew. Chem. Int. Ed. 51 (2012) 6255.
[10] P. Pulay, G. Fogarasi, G. Pongor, J.E. Boggs, A.A. Vargha, J. Am. Chem. Soc. 105 (24) (1983) 7037.
[11] A.E. Reed, L.A. Curtis, F. Weinhold, Chem. Rev. 88 (6) (1988) 899.
[12] R.F.W. Bader, Atoms in Molecules, A Quantum Theory, Oxford University Press, Oxford, 1990. ISBN: 0198558651.
[13] F. Biegler-Köning, J. Schönbohm, D. Bayles, J. Comput. Chem. 22 (2001) 545.
[14] A.D. Becke, J. Chem. Phys. 98 (7) (1993) 5648.

[15] C. Lee, W. Yang, R.G. Parr, Phys. Rev. B 37 (2) (1988) 785.
[16] (a) J.P. Perdew, K. Burke, M. Ernzerhof, Phys. Rev. Lett. 77 (1996) 3865;
(b) J.P. Perdew, Phys. Rev. B 33 (1986) 8822.
[17] E. Romano, N.A.J. Soria, R. Rudyk, S.A. Brandán, Mol. Simulat. 38 (7) (2012) 561.
[18] A.E. Ledesma, C. Contreras, J. Svoboda, A. Vektariane, S.A. Brandán, J. Mol. Struct. 967 (2010) 159.
[19] S.A. Brandán, E. Eroğlu, A.E. Ledesma, O. Oltulu, O.B. Yalçınkaya, J. Mol. Struct. 993 (2011) 225.
[20] L.C. Bichara, H.E. Lanús, C.G. Nieto, S.A. Brandán, J. Phys. Chem. A 114 (2010) 4997.
[21] C.D. Contreras, A.E. Ledesma, H.E. Lanús, J. Zinczuk, S.A. Brandán, Vib. Spectrosc. 57 (2011) 108.
[22] C.D. Contreras, A.E. Ledesma, J. Zinczuk, S.A. Brandán, Spectrochim. Acta Part A 79 (2011) 1710.
[23] P. Leyton, J. Brunet, V. Silva, C. Paipa, M.V. Castillo, S.A. Brandán, Spectrochim. Acta Part A 88 (2012) 162.
[24] E. Romano, A.B. Raschi, A. Benavente, S.A. Brandán, Spectrochim. Acta Part A 84 (2011) 111.
[25] T. Sundius, Vib. Spectrosc. 29 (2002) 89.
[26] A.B. Nielsen, A.J. Holder, GaussView, Useŕs Reference, GAUSSIAN, Inc., Pittsburgh, PA, USA, 2000–2003.
[27] E.D. Glendening, A.E. Reed, J.E. Carpenter, F. Weinhold, NBO Version 3.1. Theoretical Chemistry Institute, University of Wisconsin; Madison, WI, 1996.
[28] M.J. Frisch, G.W. Trucks, H.B. Schlegel, G.E. Scuseria, M.A. Robb, J.R. Cheeseman, J.A. Montgomery Jr., T. Vreven, K.N. Kudin, J.C. Burant, J.M. Millam, S.S. Iyengar, J. Tomasi, V. Barone, B. Mennucci, M. Cossi, G. Scalmani, N. Rega, G.A. Petersson, H. Nakatsuji, M. Hada, M. Ehara, K. Toyota, R. Fukuda, J. Hasegawa, M. Ishida, T. Nakajima, Y. Honda, O. Kitao, H. Nakai, M. Klene, X. Li, J.E. Knox, H.P. Hratchian, J.B. Cross, V. Bakken, C. Adamo, J. Jaramillo, R. Gomperts, R.E. Stratmann, O. Yazyev, A.J. Austin, R. Cammi, C. Pomelli, J.W. Ochterski, P.Y. Ayala, K. Morokuma, G.A. Voth, P. Salvador, J.J. Dannenberg, V.G. Zakrzewski, S. Dapprich, A.D. Daniels, M.C. Strain, O. Farkas, D.K. Malick, A.D. Rabuck, K. Raghavachari, J.B. Foresman, J.V. Ortiz, Q. Cui, A.G. Baboul, S. Clifford, J. Cioslowski, B.B. Stefanov, G. Liu, A. Liashenko, P. Piskorz, I. Komaromi, R.L. Martin, D.J. Fox, T. Keith, M.A. Al Laham, C.Y. Peng, A. Nanayakkara, M. Challacombe, P.M.W. Gill, B. Johnson, W. Chen, M.W. Wong, C. Gonzalez, J.A. Pople, Gaussian 03, Revision B.01, Gaussian, Inc., Wallingford, CT, 2004.
[29] A.E. Ledesma, J. Zinczuk, A. Ben Altabef, J.J. López González, S.A. Brandán, J. Raman Spectrosc. 40 (2009) 1004.
[30] J. Zinczuk, A.E. Ledesma, S.A. Brandán, O.E. Piro, J.J. López-González, A. Ben Altabef, J. Phys. Org. Chem. 22 (2009) 1166.
[31] L.A. Kristiansen, J. Krogh-Moe, J. Phys. Chem. 9 (1968) 96.
[32] S. Rada, E. Culea, M. Neumann, J. Mol. Model. 16 (8) (2010) 1333.
[33] M.M. Ilczyszyn, J. Mol. Struct. 519 (2000) 257.
[34] A. Periasamy, S. Muruganand, M. Palaniswamy, Rasayan J. Chem. 2 (4) (2009) 981.
[35] J.T. Kloprogge, R.D. Schuiling, Z. Ding, L. Hickey, H. Ruan, D. Wharton, R.L. Frost, Vib. Spectrosc. 28 (2002) 209.
[36] P. Dawson, M.M. Hargrjzave, G.R. Wilkinson, Spetrochim. Acta 33A (1977) 83.
[37] E. Knittle, W. Phillips, Q. Williams, Phys. Chem. Miner. 28 (2001) 630.
[38] K. Nakamoto, Infrared and Raman Spectra of Inorganic and Coordination Compounds, fifth ed., J. Wiley & Sons, Inc., 1997.
[39] (a) G. Rauhut, P. Pulay, J. Phys. Chem. 99 (1995) 3093;
(b) G. Rauhut, P. Pulay, Erratumml J. Phys. Chem. 99 (1995) 14572.